minerals

MDPI

Article

Effect of Fe_2O_3 Content and Acid on the Leaching Behavior of Phosphorus from Dephosphorization Slag

Shi-Wei Liu [1], Ping-Ping Li [2], Chuan-Ming Du [3,*] and Ning-Ning Lv [4]

[1] School of Metallurgical Engineering, Xi'an University of Architecture and Technology, Xi'an 710055, China; liushiw2020@xauat.edu.cn
[2] Steelmaking Plant of Beijing Shougang Co., Ltd., No. 25 Zhao'an Street, Western Industrial Zone, Qian'an, Tangshan 064400, China; lipingping6200@gmail.com
[3] School of Metallurgy, Northeastern University, Shenyang 110819, China
[4] School of Metallurgical Engineering, Anhui University of Technology, Maanshan 243032, China; lvning198565@163.com
* Correspondence: duchuanming@smm.neu.edu.cn; Tel.: +86-155-2418-9830

Abstract: Dephosphorization slag contains considerable quantities of valuable components, such as P_2O_5 and FeO_x. To recover P from dephosphorization slag, selective leaching has been adopted to separate the P-concentrating mineral phase. In this study, the effect of Fe_2O_3 content in slag and acid on the leaching behavior of P from dephosphorization slag was investigated. It was found that a higher Fe_2O_3 content in slag resulted in a higher P_2O_5 content in the C_2S–C_3P solid solution. Increasing the Fe_2O_3 content in slag promoted the dissolution of P and simultaneously suppressed the dissolution of other elements, facilitating the selective leaching of P. In the hydrochloric acid solution, more than 81% of P could be dissolved from dephosphorization slag at pH 4, and the dissolution ratio of Fe was nearly zero, achieving excellent selective leaching. Although better selective leaching was also realized in the citric acid solution at pH 5, hydrochloric acid was considered the appropriate leaching agent from the perspective of leaching cost. Through selective leaching, almost all the C_2S–C_3P solid solution was dissolved from dephosphorization slag, and the Fe-bearing matrix phase and magnesioferrite remained in the residue. The residue with low P_2O_5 content can be reutilized in ironmaking or steelmaking processes.

Keywords: dephosphorization slag; leaching; phosphorus; C_2S–C_3P solid solution

check for updates

Citation: Liu, S.-W.; Li, P.-P.; Du, C.-M.; Lv, N.-N. Effect of Fe_2O_3 Content and Acid on the Leaching Behavior of Phosphorus from Dephosphorization Slag. *Minerals* **2021**, *11*, 972. https://doi.org/10.3390/min11090972

Academic Editors: Basak Anameric and Timothy C. Eisele

Received: 10 August 2021
Accepted: 3 September 2021
Published: 7 September 2021

1. Introduction

Due to the shortage of natural resources and the deterioration of the ecological environment, the recovery of valuable components from metallurgical wastes and by-products is attracting increasing attention [1]. Dephosphorization slag, a major by-product of the steelmaking process, is generated from the dephosphorization of hot metal by adding metallurgical fluxes. The productivity of dephosphorization slag is approximately 0.10~0.15 tons per ton of molten steel [2]. Due to the enormous output of steel in China, the disposal and utilization of such large amounts of dephosphorization slag has become a crucial problem for the iron and steel industry [3]. Dephosphorization slag was principally composed of a CaO–SiO_2–FeO_x–P_2O_5 slag system and its slag basicity was lower than that of traditional converter slag [4]. At present, dephosphorization slag is normally applied as a concrete material or in road construction and landfills [5,6]. However, these applications are limited, and it is difficult to achieve the large-scale utilization of dephosphorization slag.

Dephosphorization slag contains considerable quantities of valuable components, such as FeO_x, MnO, and CaO, and its ideal utilization approach is via recycling in ironmaking or steelmaking processes as a flux [7]. However, the existence of P_2O_5 in slag hinders its recycling because phosphorus (P) is one of the most detrimental impurities in steels and the recycling of dephosphorization slag will lead to P enrichment in hot metal [8]. To achieve

its resource utilization and exploit its potential value, it is necessary to separate P from dephosphorization slag. From another perspective, P is a nutrient element and a significant ingredient in fertilizers [9]. If the separation of P from dephosphorization slag becomes technically feasible, P could be developed as a new resource, and the P-removal slag could be effectively utilized in metallurgical processes, which would not only recover the valuable components but also drastically reduce the amounts of slag generated. Therefore, separation of P from dephosphorization slag is considerably significant to both the steel and phosphate industries.

In slag, the dephosphorization product of $3CaO{\cdot}P_2O_5$ reacts with $2CaO{\cdot}SiO_2$ to form a $2CaO{\cdot}SiO_2$–$3CaO{\cdot}P_2O_5$ (C_2S–C_3P) solid solution [10]. The high distribution ratio of P_2O_5 between solid solution and other mineral phases indicates that the majority of P_2O_5 is concentrated in the C_2S–C_3P solid solution. The slag composition has a significant influence on the P_2O_5 enrichment [11,12]. Accordingly, the separation of P substantially depends on the separation of the P-concentrating solid solution from slag. Based on the difference in properties between C_2S–C_3P solid solution and other mineral phases, various methods have been proposed to treat dephosphorization slag [13]. Ono et al. [14] used the floatation of molten slag to recover the P-bearing mineral phase with low density. Miki et al. [15] studied the separation of C_2S–C_3P solid solution and the FeO-bearing liquid phase by capillary action in sintered CaO. Li et al. [16] adopted super gravity to make the P-concentrating solid solution gather in the upper molten slag.

Because the solubility of C_2S–C_3P solid solution in water is higher than that of other mineral phases, it is possible to separate the C_2S–C_3P solid solution from slag by acid leaching [17]. Compared to the above pyrometallurgical methods, the hydrometallurgical method had an advantage in terms of effectiveness and cost. Numata et al. [18] investigated the dissolution behavior of the quenched slag of a CaO–SiO_2–Fe_2O_3–P_2O_5 system in a nitric acid solution at pH 3, proving that C_2S–C_3P solid solution was dissolved selectively, although the P dissolution ratio was not high. Qiao et al. [19] used a buffer solution of $C_6H_8O_7$–NaOH–HCl to leach P from dephosphorization slag and found that the majority of P was dissolved, whereas approximately 30% of Fe was also dissolved. Lv et al. [2] studied the dissolution behavior of P from quenched dephosphorization slag with different compositions. To promote the selective leaching of P, in previous studies, slow cooling, Na_2O modification, and oxidization were proposed to treat molten dephosphorization slag [20–22]. When a citric acid solution was used, the dissolution ratio of P from slag could exceed 80%, and the dissolution of Fe was not apparent [23].

To achieve excellent selective leaching of P in at low cost, the utilization of cheap inorganic acid as a leaching agent should be considered. In addition, due to the differences in the conversion process, the composition of dephosphorization slag varies in each plant, especially the Fe_2O_3 content. To promote the utilization of acid leaching in slag treatment, the leaching behavior of P from dephosphorization slag with different levels of Fe_2O_3 content was investigated in dilute citric acid and hydrochloric acid solutions, respectively.

2. Experimental

Reagent-grade MnO, MgO, Fe_2O_3, $Ca_3(PO_4)_2$, SiO_2, and CaO were utilized to fabricate the dephosphorization slag, which was similar to practical slag. In this study, Fe_2O_3 was selected as the iron oxide because the dissolution ratio of P was relatively high when Fe_2O_3 existed [22]; CaO was produced by calcining $CaCO_3$ at 1273 K for 10 h. Table 1 lists the composition of three kinds of dephosphorization slag. These types of slag have the same P_2O_5 content and basicity (%CaO/%SiO_2). To investigate the effect of Fe_2O_3, the Fe_2O_3 content ranged from 24.0% to 36.0%. According to the slag composition, the mixture of reagents was fully mixed and placed in a Pt crucible. The sample was first heated to 1823 K to form a liquid slag in a $MoSi_2$ resistance furnace. After maintaining this temperature for 30 min, the molten slag was cooled to 1623 K at a speed of 3 K/min to precipitate the C_2S–C_3P solid solution. Then, the sample was cooled to 1273 K and taken out of the furnace. After cooling, the sample was crushed and sieved to a particle size of less than

53 μm to promote the dissolution of P in the following experiments. The composition and morphology of the mineral phases in the dephosphorization slag were analyzed by X-ray diffraction (XRD) (Rigaku Corporation, Tokyo, Japan) and electron probe microanalysis (EPMA) (JEOL, Tokyo, Japan).

Table 1. Composition of dephosphorization slag with different Fe_2O_3 content (mass%).

	CaO	SiO_2	Fe_2O_3	P_2O_5	MgO	MnO
Slag 1	40.7	25.3	24.0	3.0	4.0	3.0
Slag 2	36.7	22.8	30.5	3.0	4.0	3.0
Slag 3	33.3	20.7	36.0	3.0	4.0	3.0

Leaching experiments were conducted in a Teflon container with 300 mL of distilled water, which was immersed in a constant-temperature water bath at 298 K. The leaching parameters were determined based on previous studies [20–23]. First, 1.5 g of slag was added to the distilled water and the solution was agitated by a rotating stirrer. The dissolution of Ca from slag resulted in an increase in pH. To achieve the selective leaching of P, the pH of the solution was controlled at a constant value. Hence, dilute acid solution was automatically added to decrease the pH of aqueous solution by a PC control system. In this study, hydrochloric acid (HCl) solution (0.4 mol/L) was selected as the leaching agent and compared with citric acid solution (0.2 mol/L). The leaching experiments were conducted at pH 4 and 5, respectively. At appropriate intervals, approximately 4 mL of solution was withdrawn and filtered by a membrane filter (<0.45 μm). The concentration of each element in the filtered solution was analyzed using inductively coupled plasma atomic emission spectroscopy (ICP-AES) (SPECTRO, Kleve, Germany). After 120 min, the residue was separated from the solution by vacuum filtration. Following drying, the mass of residue was weighted, and its morphology and mineral composition were characterized by EPMA and XRD. After performing aqua-regia digestion, the chemical composition of residue was determined by ICP-AES analysis.

The dissolution ratio of element M (R_M) from dephosphorization slag was calculated using the element concentration in the solution, as expressed in Equation (1):

$$R_M = \frac{C_M \cdot V}{m_M} \tag{1}$$

where C_M is the M concentration in the solution (mg/L); V is the final volume of solution (L); m_M is the mass of M in slag (mg).

3. Results

3.1. Mineralogical Composition

Figure 1 presents the morphology of the mineral phases in dephosphorization slag with different amounts of Fe_2O_3 content. The average composition of each mineral phase is listed in Table 2. Three kinds of mineral phases were distinctly observed in each slag. It is worth noting that the area ratios of the mineral phases in each slag were different. The white phase had a net structure, and some dark gray phase was wrapped in it. The white phase rich in Fe_2O_3 was considered the magnesioferrite. The light gray phase consisting of the CaO–SiO_2–Fe_2O_3 slag system was regarded as the matrix phase, which had low P_2O_5 content. The dark gray phase primarily consisted of CaO and SiO_2, and it had a relatively high P_2O_5 content compared to other mineral phases. This phase was considered the C_2S–C_3P solid solution. As reported in a previous study [11], there was a high distribution ratio of P_2O_5 between the solid solution and matrix phase, demonstrating that P_2O_5 was enriched. Fe_2O_3 was mainly distributed in the matrix phase and magnesioferrite. Most of the MgO and MnO was distributed in the magnesioferrite. Because P_2O_5 and Fe_2O_3 were concentrated in different mineral phases, this provided an opportunity to separate P and Fe.

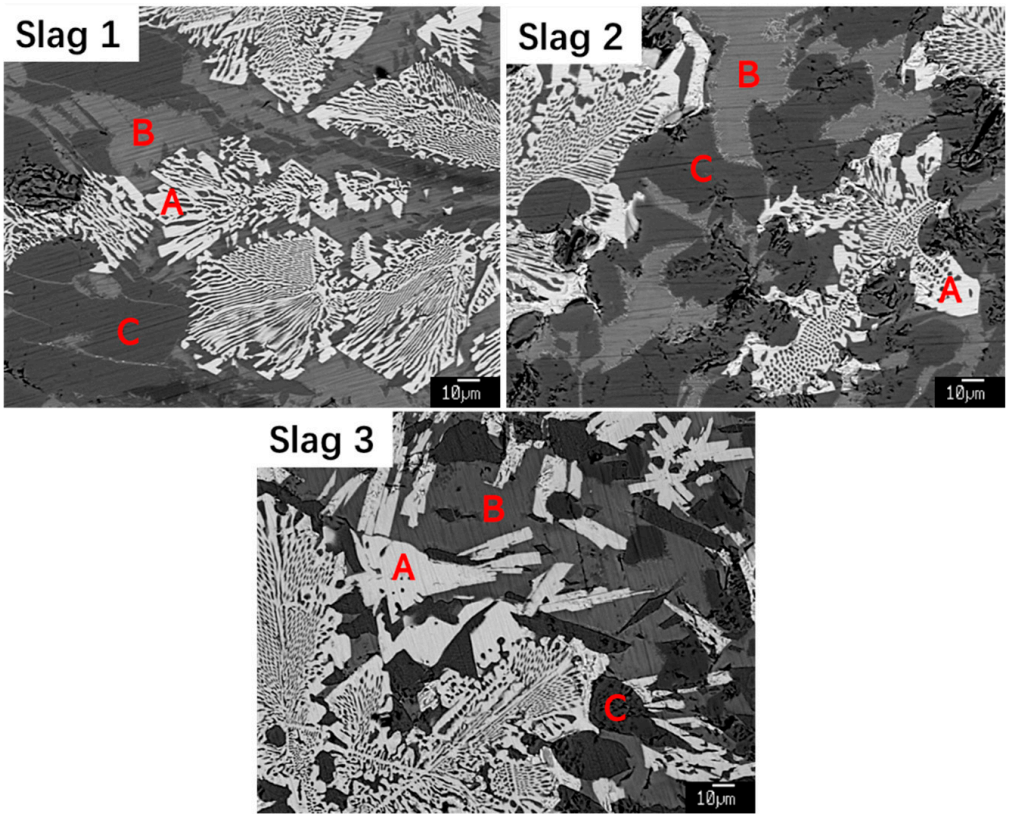

Figure 1. Morphology of dephosphorization slag with different amounts of Fe_2O_3 content. A,B,C: analysis point. Its composition is described in Table 2.

Table 2. Composition of mineral phases in different types of dephosphorization slag (mass%).

Mineral Phase		CaO	SiO_2	Fe_2O_3	P_2O_5	MgO	MnO
Slag 1	A	1.4	0.2	76.5	0.0	12.8	9.1
	B	32.6	31.1	33.1	0.6	1.2	1.4
	C	59.9	29.7	1.8	7.1	0.8	0.7
Slag 2	A	2.3	0.1	78.2	0.0	10.4	9.0
	B	32.2	31.8	33.8	0.5	0.9	0.8
	C	59.7	28.4	1.9	9.2	0.4	0.4
Slag 3	A	2.1	0.1	79.1	0.0	9.9	8.8
	B	31.5	33.4	33.2	0.4	0.8	0.7
	C	59.5	27.4	1.6	10.8	0.4	0.3

As the Fe_2O_3 content in slag increased, the P_2O_5 content in the C_2S–C_3P solid solution increased, indicating that P_2O_5 was further enriched. The P_2O_5 content in the solid solution could reach 10.8%, approximately 3.6 times higher than that in slag 3. The composition of the matrix phase had little change. The Fe_2O_3 content in the magnesioferrite increased with the Fe_2O_3 content in the slag. As shown in Figure 1, in the case of high Fe_2O_3 content, the area ratio of solid solution was lower than that in slag 1, illustrating that increasing Fe_2O_3 content was not beneficial for the formation of C_2S–C_3P solid solution. It was considered that a part of CaO and SiO_2 in the solid solution reacted with the excess Fe_2O_3. Due to the decrease in mass fraction, the P_2O_5 content in the C_2S–C_3P solid solution increased.

3.2. Leaching Results

The dissolution behavior of each dephosphorization slag in the hydrochloric acid solution at pH 4 is shown in Figure 2. The concentrations of the main elements in the

solution increased continuously with leaching time. In the beginning, the dissolution of Ca, Si, and P from slag was very fast, resulting in higher concentrations in 20 min, indicating that the C_2S–C_3P solid solution was dissolved easily. The dissolution rate of slag gradually decreased, and the concentrations of the main elements showed a slight increase after 60 min. The Ca concentration was the highest among the dissolved elements, while the Fe concentration was very low in each case, illustrating that the dissolution of Fe-bearing mineral phases was difficult. A higher Fe_2O_3 content in slag led to lower Ca and Si concentrations in the solution. When the Fe_2O_3 content increased from 24.0% to 36.0%, the Ca concentration decreased from 1100.3 mg/L to 841.7 mg/L after 120 min. The Si concentrations from slag 2 and 3 were very similar, approximately 130 mg/L after 120 min. This is because the mass fraction of C_2S–C_3P solid solution was lower in the slag with high Fe_2O_3 content. Contrary to Ca and Si, the P concentration in the solution increased significantly with the Fe_2O_3 content in slag. For slag 3, the P concentration reached 49.7 mg/L. Due to the extremely low Fe concentration, the P-containing solution is suitable for phosphorus recovery. It has been reported that calcium phosphates could be extracted from this kind of solution by chemical precipitation [23].

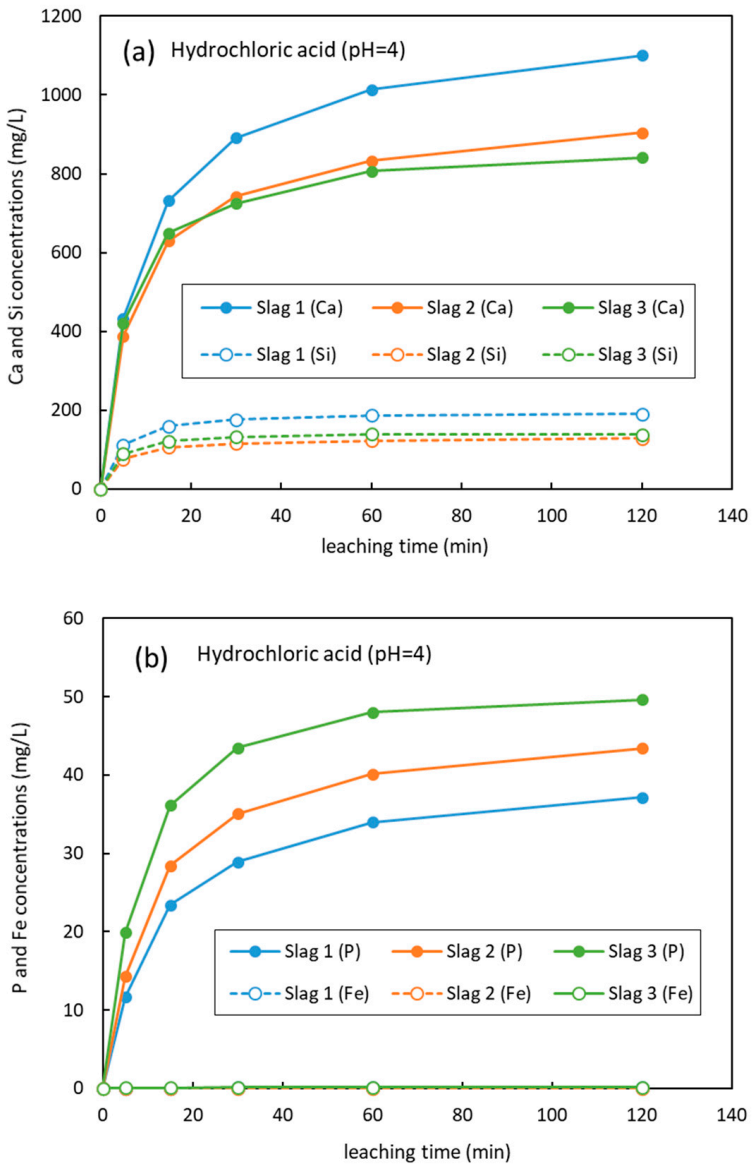

Figure 2. (**a**) Change in the Ca and Si concentrations with time in the hydrochloric acid solution; (**b**) Change in the P and Fe concentrations with time in the hydrochloric acid solution.

Figure 3 shows the dissolution ratio of each element from dephosphorization slag in the hydrochloric acid solution at pH 4. The dissolution ratios of Ca, Si, and P were far higher than those of Fe, Mg, and Mn. In particular, Fe could hardly dissolve from each slag. For slag 1 with low Fe_2O_3 content, most of the Ca was dissolved, and the dissolution ratio of Si was 35.0%, higher than that of other slags. The dissolution of Mg and Mn indicated that a small part of the matrix phase or magnesioferrite was also dissolved. However, only 61.2% of P was dissolved from this slag, and the dissolution ratio of Fe was nearly zero. It was considered that the Fe^{3+} ions dissolved from slag reacted with phosphate ions to form ferric phosphate. As expressed in Equation (2), the equilibrium constant of this reaction (K) is high, indicating that this reaction can occur easily [24]. Increasing the Fe_2O_3 content in slag suppressed the dissolution of each element except for P. More than 81% of P was dissolved from slag 3, and the dissolution ratios of Mg and Mn were less than 5%, achieving excellent selective leaching. This result illustrated that the majority of the C_2S–C_3P solid solution was dissolved, without significant dissolution of other mineral phases.

$$Fe^{3+} + HPO_4^{2-} + 2H_2O = FePO_4 \cdot 2H_2O + H^+ \quad log\ K = 13.71 \tag{2}$$

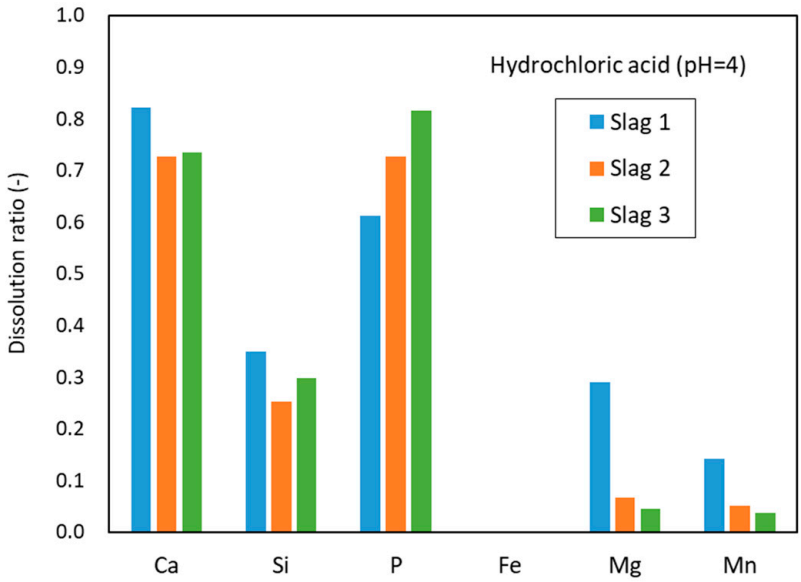

Figure 3. Dissolution ratio of each element from dephosphorization slag in hydrochloric acid solution at pH 4.

The dissolution behavior of P and Fe from dephosphorization slag in hydrochloric acid solution at pH 5 was compared with the results at pH 4, as shown in Figure 4. Increasing the pH significantly decreased the dissolution ratio of P, while it had no influence on the dissolution of Fe. This is because the dissolution of C_2S–C_3P solid solution became difficult when the concentration of H^+ ions lowered. In addition, the phosphate ions dissolved from slag were easier to precipitate at a higher pH condition. At pH 5, the variation trend of P dissolution was the same as that at pH 4. The dissolution ratio of P increased with the Fe_2O_3 content in slag. However, only 68.2% of P was dissolved from slag 3. In summary, a higher Fe_2O_3 content and lower pH was beneficial for the dissolution of P from dephosphorization slag.

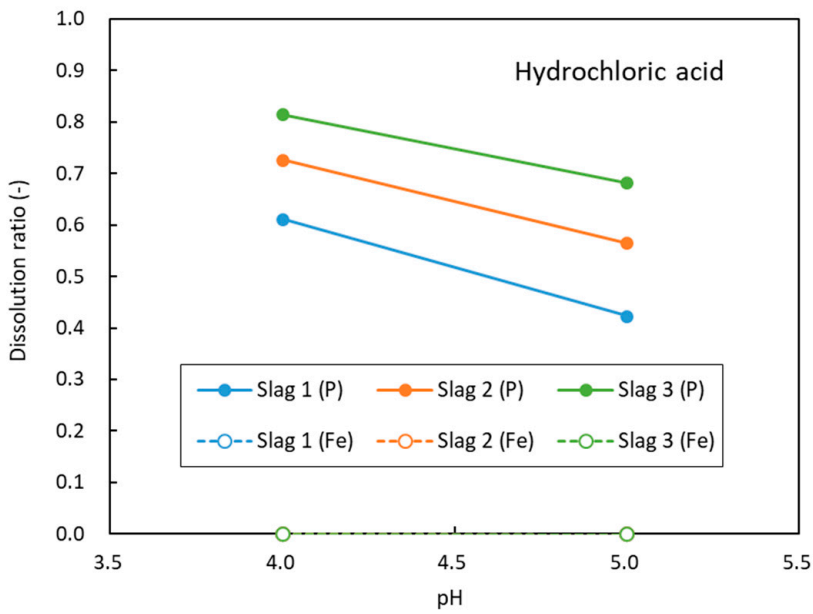

Figure 4. Dissolution ratio of each element from dephosphorization slag in hydrochloric acid solution at various pH conditions.

Citric acid was commonly used as a leaching agent in previous studies [21–23]. To understand the effect of acid and select an appropriate leaching agent, the dissolution behavior of dephosphorization slag with different amounts of Fe_2O_3 content in citric acid solution was also investigated. Figure 5 shows the dissolution ratio of each element from slag at pH 4. Compared to the leaching results in Figure 3, dephosphorization slag was easier to dissolve in the citric acid solution. Almost all the Ca, Si, and P was dissolved, and the dissolution ratios of Fe, Mn, and Mg were relatively high. In the citric acid solution, citrate ions ($C_6H_5O_7^{3-}$) could combine with Ca^{2+} and Fe^{3+} ions to form complexes [25]. It has been reported that the formation of complexes on the surface of the mineral phase shifts the electron density toward the metal ion, which destabilizes the crystal lattice and facilitates the detachment of metal ions into aqueous solutions [26]. Therefore, citric acid was more effective to dissolve slag, resulting in a higher dissolution ratio of each element. As the Fe_2O_3 content in slag increased, the dissolution ratio of P increased slightly, while those of other elements decreased. The dissolution ratios of P and Fe from slag 3 were 96.7% and 21.7%, respectively, illustrating that a part of the Fe-containing mineral phases was also dissolved.

Figure 6 shows the dissolution ratios of P and Fe from dephosphorization slag in the citric acid solution at pH 4 and 5. The dissolution ratio of P decreased slightly when the pH increased from 4 to 5, indicating that most of the P-concentrating solid solution was still dissolved under this condition. The dissolution ratio of P from slag 3 was 91.3% at pH 5. Increasing the pH significantly decreased the dissolution ratio of Fe, indicating that the dissolution of Fe-bearing mineral phases was suppressed. The dissolution ratio of Fe from slag 3 decreased approximately seven times, only 2.9% at pH 5. This illustrates that better selective leaching of P was also realized in the citric acid solution at pH 5.

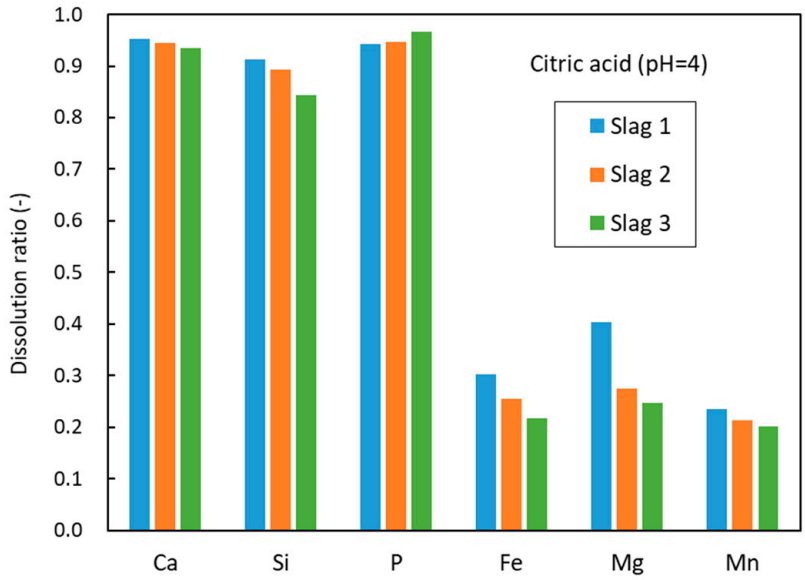

Figure 5. Dissolution ratio of each element from dephosphorization slag in citric acid solution at pH 4.

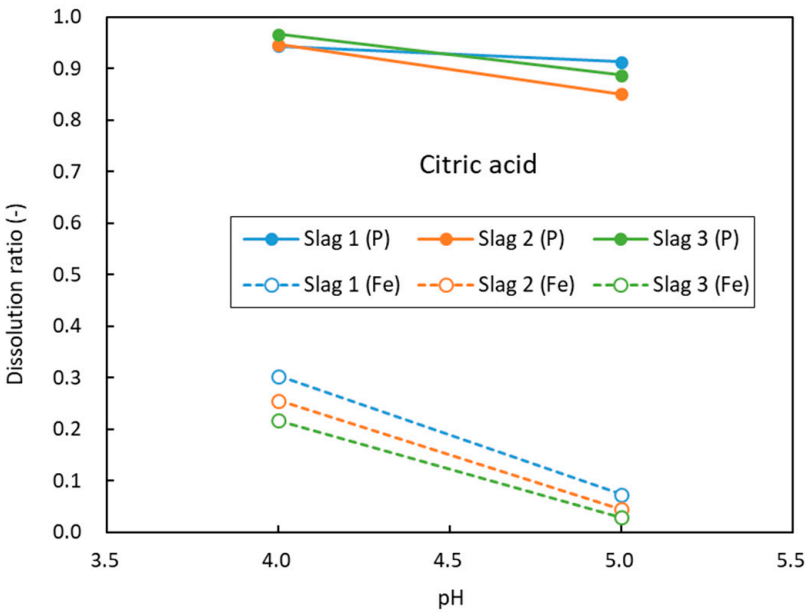

Figure 6. Dissolution ratio of each element from dephosphorization slag in citric acid solution at various pH conditions.

In summary, increasing the Fe_2O_3 content in slag promoted the dissolution of P and simultaneously suppressed the dissolution of other elements. Better selective leaching of P from dephosphorization slag was achieved in the hydrochloric acid solution at 4. Although the dissolution ratio of P was slightly lower than that in the citric acid solution, the dissolution ratio of Fe was negligible in the hydrochloric acid solution. From the perspective of treatment cost, hydrochloric acid was considered an appropriate leaching agent.

4. Discussions

To understand the dissolution behavior of mineral phases, the mass fractions of mineral phases in dephosphorization slag were compared with those of the dissolved slag

and residue. Using the composition of mineral phases, their mass fractions were calculated based on the mass balance of each oxide, as described in Equations (3) and (4).

$$(\%MO)_{slag} = \alpha(\%MO)_{\alpha} + \beta(\%MO)_{\beta} + \gamma(\%MO)_{\gamma} \quad (3)$$

$$\alpha + \beta + \gamma = 1 \quad (4)$$

where α, β, and γ are the mass fractions of solid solution, matrix phase, and magnesioferrite, respectively; $(\%MO)_{slag}$ is the MO content in slag; $(\%MO)_{\alpha}$ is the MO content in the solid solution.

The mass fraction of dissolved slag was calculated using the dissolution ratio of each element. Figure 7 presents the mass fractions of mineral phases and dissolved slag in the hydrochloric acid solution at pH 4. In slag 1 with low Fe_2O_3 content, the mass fraction of solid solution was approximately 47%, and that of magnesioferrite was relatively low. With the increase in Fe_2O_3 content, the mass fraction of solid solution decreased, while that of magnesioferrite increased. This result was consistent with the EPMA analysis. There was no significant change in the mass fraction of the matrix phase. The mass fraction of dissolved slag decreased with the increase in Fe_2O_3 content. In each case, the mass fraction of dissolved slag was slightly lower than that of the solid solution. Because the C_2S–C_3P solid solution was readily dissolved, it was found that a large amount of the C_2S–C_3P solid solution was dissolved and separated from slag. However, the dissolution ratio of P from slag 1 was not high, and a part of Mg and Mn was also dissolved. As discussed above, it is considered that a part of the P dissolved from the solid solution was precipitated with Fe^{3+} ions dissolved from slag under this condition. For slag 3, the dissolution ratio of P was the highest, illustrating that almost all the C_2S–C_3P solid solution was dissolved and the phosphate precipitation was not significant.

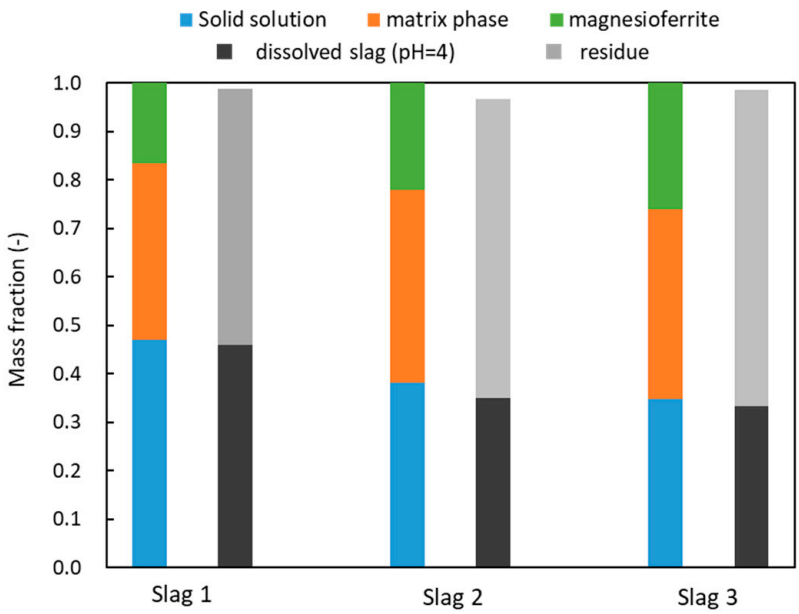

Figure 7. Mass fractions of mineral phases compared with that of dissolved slag in hydrochloric acid solution at pH 4.

Figure 8 shows the mass fractions of dissolved slag in the citric acid solution at pH 4. A large amount of slag was dissolved in the citric acid solution, and the dissolution of slag became difficult as the Fe_2O_3 content increased. Due to the large dissolution of slag, acid consumption was high during leaching. Approximately 60.9% of slag 3 was dissolved, and this value was far higher than the mass fraction of solid solution. This indicated that the C_2S–C_3P solid solution was sufficiently dissolved and a part of the matrix phase and

magnesioferrite was also dissolved. Although the Fe^{3+} concentration in the solution was high, most of the Fe^{3+} ions formed complexes with citrate ions. The precipitation of ferrite phosphate was avoided in the citric acid solution. Therefore, almost all the P was dissolved from slag, even with a higher dissolution ratio of Fe.

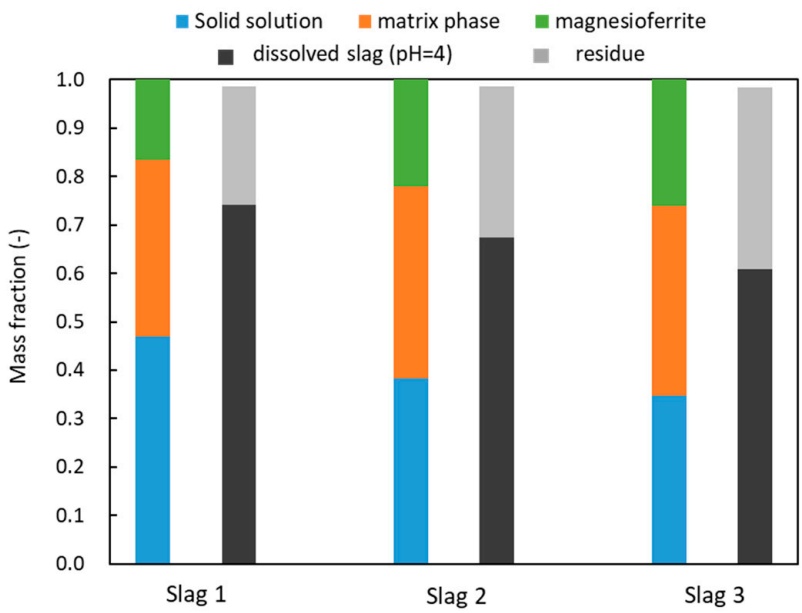

Figure 8. Mass fractions of mineral phases compared with that of dissolved slag in citric acid solution at pH 4.

Based on the mass fractions of mineral phases, the mass ratios of P and Fe distributed in the C_2S–C_3P solid solution were calculated. These results were compared with the dissolution ratios of P and Fe in the hydrochloric acid solution at pH 4, as shown in Figure 9. More than 93.7% of P was distributed in the C_2S–C_3P solid solution, while the mass ratio of Fe was less than 3.3%. If the C_2S–C_3P solid solution was totally dissolved and no precipitation occurred, the dissolution ratio should be equal to the mass ratio. However, there was a large difference between the mass ratio of P and the dissolution ratio of P. With the increase in Fe_2O_3 content, this difference became smaller. The variation trend of Fe was the same. Because most of the C_2S–C_3P solid solution was dissolved, it demonstrated that some of the phosphate ions precipitated with Fe^{3+} ions in the hydrochloric acid solution. In the case of high Fe_2O_3 content, due to the low dissolution ratio of Fe, phosphate precipitation could be suppressed.

Table 3 lists the average composition of residues after leaching in hydrochloric acid solution at pH 4. Compared to the original slag composition, the P_2O_5 content in the residue decreased while the Fe_2O_3 content increased. A higher Fe_2O_3 content in slag resulted in a lower P_2O_5 content in the residue. The residue of slag 3 contained only 0.7% P_2O_5, demonstrating effective separation of P and Fe. This P-removal residue had a high Fe_2O_3 content, which can substitute for iron ores.

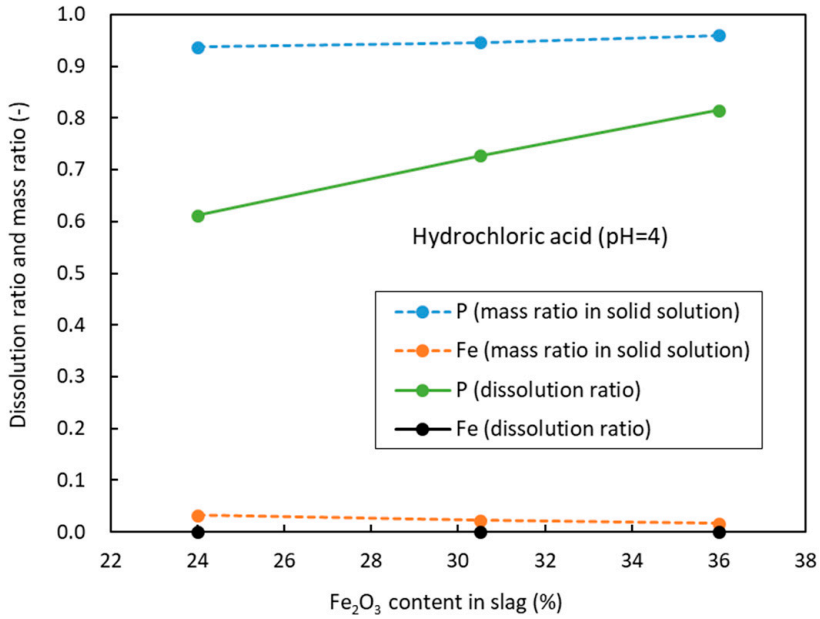

Figure 9. Dissolution ratio of P from different types of dephosphorization slag and the mass ratio of P in the solid solution.

Table 3. Composition of residues after leaching in hydrochloric acid solution at pH 4 (mass%).

	CaO	SiO_2	P_2O_5	Fe_2O_3	MgO	MnO
Residue (slag 1)	10.0	32.3	2.1	45.5	5.0	5.1
Residue (slag 2)	11.6	27.4	0.9	50.4	5.1	4.6
Residue (slag 3)	11.4	22.7	0.7	56.5	4.5	4.2

Because slag 3 showed better selective leaching at pH 4, the mineralogical composition and morphology of its residue were analyzed. Figure 10 shows the XRD patterns of slag 3 and its residue. The characteristic peaks of C_2S–C_3P solid solution and magnesioferrite were observed in the original slag. Because the matrix phase was an amorphous glass phase, it had no characteristic peaks. After leaching, the peaks of C_2S–C_3P solid solution almost disappeared, while the peaks of magnesioferrite intensified. This further demonstrated that the P-concentrating solid solution was separated from the slag and the Fe-bearing mineral phases remained in the residue.

Figure 11 shows the morphology of the residue after leaching in the hydrochloric acid solution. The composition of the identified domains on the residue surface is listed in Table 4. Two mineral phases, similar to the matrix phase and magnesioferrite, were observed. It was difficult to detect the C_2S–C_3P solid solution. This shows that the residue principally comprised the matrix phase and magnesioferrite after the separation of the solid solution, which can be reutilized as a raw material in ironmaking or steelmaking processes. In this study, effective selective leaching of P was realized, which would promote the resource utilization of dephosphorization slag.

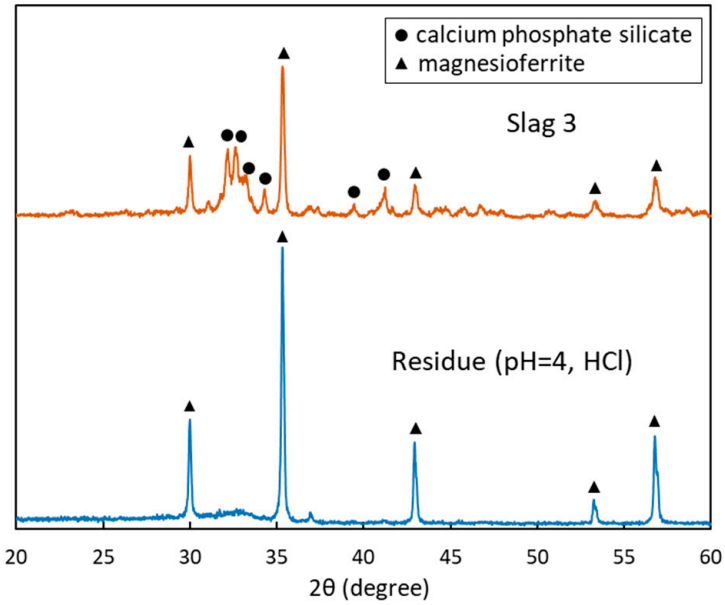

Figure 10. XRD patterns of slag 3 and its residue after leaching in hydrochloric acid solution at pH 4.

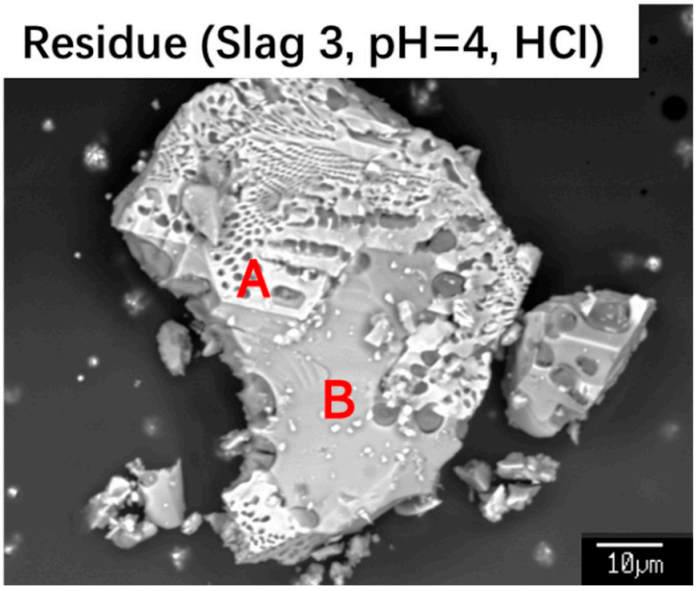

Figure 11. Morphology of residue after leaching in hydrochloric acid solution at pH 4. A,B: analysis point. Its composition is shown in Table 4.

Table 4. Composition of mineral phases on the residue surface (mass%).

Point	Ca	Si	Fe	P	Mg	Mn
A	1.3	0	55.1	0	5.8	6.4
B	22.6	15.2	23.0	0.2	0.4	0.5

5. Conclusions

The effect of Fe_2O_3 content in slag and acid on the selective leaching of P from dephosphorization slag was investigated in this study. The P_2O_5 content in the C_2S–C_3P solid solution increased with the Fe_2O_3 content in slag. Increasing the Fe_2O_3 content in slag increased the dissolution ratio of P and simultaneously suppressed the dissolution of other elements, which was beneficial for the selective leaching of P. More than 81% of P

was dissolved from dephosphorization slag in hydrochloric acid solution at pH 4, and the dissolution ratio of Fe was nearly zero, achieving excellent selective leaching. Although better selective leaching was also realized in citric acid solution at pH 5, hydrochloric acid was considered an appropriate leaching agent from the perspective of leaching cost. Almost all the C_2S–C_3P solid solution was dissolved from dephosphorization slag by acid leaching, and the Fe-bearing matrix phase and magnesioferrite remained in the residue. The residue contained 0.7% P_2O_5 and 56.5% Fe_2O_3 and can be reutilized as a flux in ironmaking or steelmaking processes.

Author Contributions: Conceptualization, C.-M.D. and S.-W.L.; methodology, C.-M.D.; investigation, P.-P.L. and S.-W.L.; resources, N.-N.L. and C.-M.D.; writing—original draft preparation, S.-W.L.; writing—review and editing, C.-M.D., P.-P.L., and N.-N.L. All authors have read and agreed to the published version of the manuscript.

Funding: This research was supported by the Fundamental Research Funds for the Central Universities (No. N2025005), and the National Natural Science Foundation of China (No. 52104326, No. 51704223, and No. 52074004).

Data Availability Statement: Data are contained within the article.

Conflicts of Interest: The authors declare no conflict of interest.

References

1. Du, C.; Gao, X.; Kitamura, S. Measures to decrease and utilize steelmaking slag. *J. Sustain. Metall.* **2019**, *5*, 141–153. [CrossRef]
2. Lv, N.; Du, C.; Kong, H.; Yu, H. Leaching of phosphorus from quenched steelmaking slags with different composition. *Metals* **2021**, *11*, 1026. [CrossRef]
3. Guo, J.; Bao, Y.; Wang, M. Steel slag in China: Treatment, recycling, and management. *Waste Manag.* **2018**, *78*, 318–330. [CrossRef]
4. Sun, H.; Yang, J.; Lu, X.; Liu, W.; Ye, G.; Zhang, R.; Yang, W. Dephosphorization in double slag converter steelmaking process at different temperatures by industrial experiments. *Metals* **2021**, *11*, 1030. [CrossRef]
5. Aponte, D.; Soto Martín, O.; Valls del Barrio, S.; Barra Bizinotto, M. Ladle steel slag in activated systems for construction use. *Minerals* **2020**, *10*, 687. [CrossRef]
6. Singh, S.K.; Rekha, P.; Surya, M. Utilization of Linz–Donawitz slag from steel industry for waste minimization. *J. Mater. Cycles Waste Manag.* **2020**, *22*, 611–627. [CrossRef]
7. Diao, J.; Zhou, W.; Ke, Z.; Qiao, Y.; Zhang, T.; Liu, X.; Xie, B. System assessment of recycling of steel slag in converter steelmaking. *J. Clean. Prod.* **2016**, *125*, 159–167. [CrossRef]
8. Matsubae, K.; Yamasue, E.; Inazumi, T.; Webeck, E.; Miki, T.; Nagasaka, T. Innovations in steelmaking technology and hidden phosphorus flows. *Sci. Total Environ.* **2016**, *542*, 1162–1168. [CrossRef]
9. Ohtake, H.; Tsuneda, S. *Phosphorus Recovery and Recycling*; Springer: Singapor, 2019.
10. Kikuchi, N.; Matsui, A.; Uchida, Y. Effect of lime dissolution rate in slag on hot metal dephosphorization. *ISIJ Int.* **2020**, *60*, 922–929. [CrossRef]
11. Yan, Z.; Deng, Z.; Zhu, M. Effect of $CaCl_2$ addition on phosphorus distribution between CaO–SiO_2–FeO_x–P_2O_5 slag and carbon-saturated iron at steelmaking temperature. *Metall. Mater. Trans. B* **2021**, *52*, 2806–2815. [CrossRef]
12. Ye, G.F.; Yang, J.; Zhang, R.H.; Yang, W.K.; Sun, H. Behavior of phosphorus enrichment in dephosphorization slag at low temperature and low basicity. *Int. J. Miner. Metall.* **2021**, *28*, 66–75. [CrossRef]
13. Wang, Z.; Sohn, I. A review on reclamation and reutilization of ironmaking and steelmaking slags. *J. Sustain. Metall.* **2019**, *5*, 127–140. [CrossRef]
14. Ono, H.; Inagaki, A.; Masui, T.; Narita, H.; Mitsuo, T.; Nosaka, S.; Gonda, S. Removal of phosphorus from LD converter slag by floating of dicalcium silicate during solidification. *Tetsu-to-Hagané* **1980**, *66*, 1317–1326. [CrossRef]
15. Miki, T.; Kaneko, S. Separation of FeO and P_2O_5 from steelmaking slag utilizing capillary action. *ISIJ Int.* **2015**, *55*, 142–148. [CrossRef]
16. Li, C.; Gao, J.; Guo, Z. Isothermal enrichment of P-concentrating phase from CaO–SiO_2–FeO–MgO–P_2O_5 melt with super gravity. *ISIJ Int.* **2016**, *56*, 759–764. [CrossRef]
17. Teratoko, T.; Maruoka, N.; Shibata, H.; Kitamura, S. Dissolution behavior of dicalcium silicate and tricalcium phosphate solid solution and other phases of steelmaking slag in an aqueous solution. *High. Temp. Mater. Processes.* **2012**, *31*, 329–338. [CrossRef]
18. Numata, M.; Maruoka, N.; Kim, S.; Kitamura, S. Fundamental experiment to extract phosphorous selectively from steelmaking slag by leaching. *ISIJ Int.* **2014**, *54*, 1983–1990. [CrossRef]
19. Qiao, Y.; Diao, J.; Liu, X.; Li, X.; Zhang, T.; Xie, B. Dephosphorization of steelmaking slag by leaching with acidic aqueous solution. *JOM* **2016**, *68*, 2511–2519. [CrossRef]
20. Du, C.; Gao, X.; Ueda, S.; Kitamura, S. A kinetic study on selective leaching of phosphorus from dephosphorization slag. *J. Sustain. Metall.* **2020**, *6*, 724–738. [CrossRef]

21. Du, C.; Gao, X.; Ueda, S.; Kitamura, S. Effect of Na_2O addition on phosphorus dissolution from steelmaking slag with high P_2O_5 content. *J. Sustain. Metall.* **2017**, *3*, 671–682. [CrossRef]
22. Du, C.; Gao, X.; Ueda, S.; Kitamura, S. Effect of Fe^{2+}/T.Fe ratio on the dissolution behavior of P from steelmaking slag with high P_2O_5 content. *J. Sustain. Metall.* **2018**, *4*, 443–454. [CrossRef]
23. Du, C.; Gao, X.; Ueda, S.; Kitamura, S. Recovery of phosphorus from modified steelmaking slag with high P_2O_5 content via leaching and precipitation. *Tetsu-to-Hagané* **2021**, *107*, 103–111. [CrossRef]
24. Futatsuka, T.; Shitogiden, K.; Miki, T.; Nagasaka, T.; Hino, M. Dissolution behavior of nutrition elements from steelmaking slag into seawater. *ISIJ Int.* **2004**, *44*, 753–761. [CrossRef]
25. Bassi, R.; Prasher, S.O.; Simpson, B.K. Extraction of metals from a contaminated sandy soil using citric acid. *Environ. Prog.* **2000**, *19*, 275–282. [CrossRef]
26. Astuti, W.; Hirajima, T.; Sasaki, K.; Okibe, N. Comparison of effectiveness of citric acid and other acids in leaching of low-grade Indonesian saprolitic ores. *Miner. Eng.* **2016**, *85*, 1–16. [CrossRef]